Journal of ELECTRICAL ENGINEERING, VOL. 57, NO. 4, 2006, 185–192

RADIAL MAGNETIC FORCES OF SINGLE–PHASE PERMANENT SPLIT–CAPACITOR MOTOR

Valéria Hrabovcová — Pavol Rafajdus *

This paper deals with investigation of radial forces developed in an unsymmetrical air-gap of a single phase induction motor to avoid noise operation. The calculation is made on the basis of magnetic field analysis by means of FEMM. It is shown that eccentricity of the air-gap has a significant negative influence on the machine operation.

K e y w o r d s: radial magnetic forces, single-phase permanent split-capacitor motor, air gap eccentricity, slot harmonics, magnetic field analysis, noise and vibration of electrical machines

1 INTRODUCTION

The aim of the paper is to investigate radial magnetic forces developed in the air-gap of a single phase induction motor (IM) with a permanent capacitor in the auxiliary phase and their dependence of the air-gap eccentricity.

It is known that the noise and vibration of the electric motors have a severe influence on the motor operation as well as on its life and reduce its reliability.

As to the primary source of noise, it can be caused by mechanical and magnetic reasons. Magnetic noise corresponds to the resonance phenomena between mechanical forces caused by the time and space variable magnetic field of the electrical machine and its mechanical parts, mainly between stator and rotor lamination stacks.

As it is known, the most serious source of magnetic noise are the so-called stator and rotor slot harmonics, which can have the following orders

$$m = g_S Q_S + p\,, \quad n = g_R Q_R + p\,. \qquad (1,2)$$

Here p is the number of pole pairs, m (n) is the order of stator (rotor) harmonics, Q_S (Q_R) is the number of stator (rotor) slots, g_S (g_R) is any positive or negative integer. Each stator harmonics of m-order creates with each rotor harmonics of n-order a radial force, acting perpendicularly on the shaft, the order of which is given as follows:

$$r = m \pm n = \big(g_S Q_S + p\big) \pm \big(g_R Q_R + p\big)\,. \qquad (3)$$

There are also other radial forces created by the stator and rotor harmonics of various orders but they are negligible in comparison with the above mentioned r-forces given by (3).

This paper deals with investigation of such radial forces in a single-phase induction motor with a permanent capacitor in the auxiliary winding and is focused on the influence of air-gap eccentricity.

2 MAGNETIC FIELD ANALYSIS

As a first step, analysis of the magnetic field in the cross section area of the investigated motor has been made by means of FEMM (Finite Element Method Magnetic — free public licence) which enables such calculations.

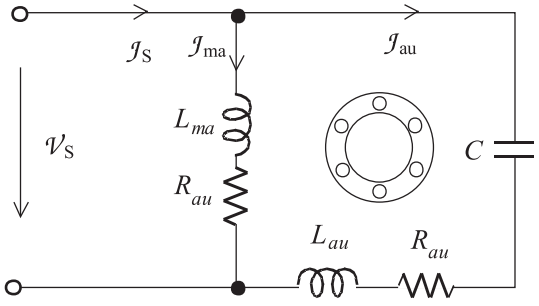

Fig. 1. Connection of the main and auxiliary windings.

Figure 1 shows the connections of main and auxiliary windings Fig. 2 shows the cross-section area with the distribution of the main (subscript "ma") and auxiliary ("au") windings in the stator slots ($Q_S = 24$, $Q_R = 30$).

In Fig. 3 there is a phasor diagram of the measured no-load current and its components and in Fig. 4 time waveforms of the main and auxiliary currents, to be able to put currents of individual instants to the FEMM program. As it is seen in this figure, the instants at which both currents have equal magnitudes are $\omega t = 74.6°$ and $254.6°$. At these instants the air-gap flux density will achieve its maximum and at instants $164.6°$ and $344.6°$ its minimum.

* Faculty of Electrical Engineering, University of Žilina, Veľký diel, 01026 Žilina, Slovakia, E-mail: Valeria.Hrabovcova@fel.utc.sk, Pavol.Rafajdus@kves.utc.sk

ISSN 1335-3632

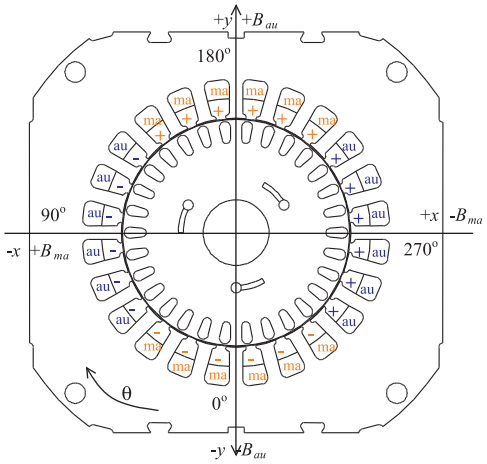

Fig. 2. Cross-section area of the investigated motor with a symmetrical air-gap.

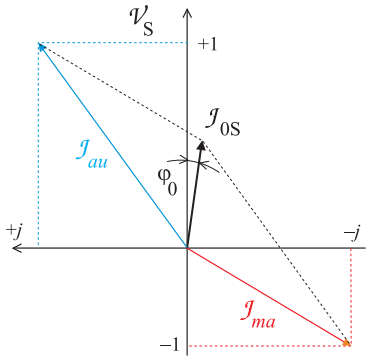

Fig. 3. Phasor diagram of measured no-load currents.

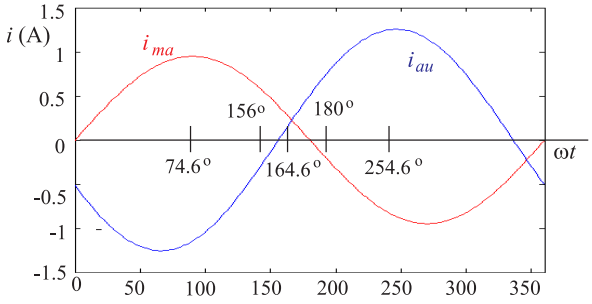

Fig. 4. Time waveforms of the main and auxiliary currents.

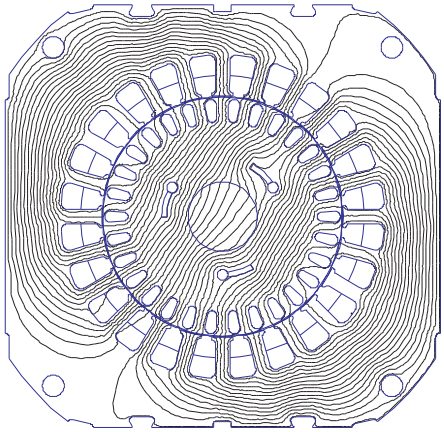

Fig. 5. A plot of magnetic flux lines.

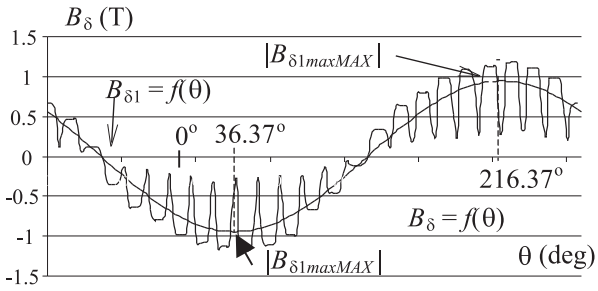

Fig. 6. Instantaneous values of air-gap flux density at current instant 74.6°.

A plot of magnetic lines is shown in Fig. 5 where it is seen that it is a two-pole machine. Instantaneous values of air-gap flux density at instant 74.6° is in Fig. 6, where one can see also the fundamental harmonic and its amplitude. Because the waveform is made at current instant 74.6°, it is its maximum possible amplitude $B_{\delta l\max \mathrm{MAX}}$, which occurs at 36.3° shifted from space origin (zero), as it is shown in Fig. 2 and Fig. 8. Space origin is placed in position, where the amplitude of magnetic flux density at current instant 0° will occur.

Such an analysis made at every instant of current waveforms enables to show Fig. 7, where amplitude $B_{\delta l\,\max}$ around the whole air-gap is seen $B_{\delta l\,\max} = f(\Theta)$. Here one can see its minimum $B_{\delta 1\max \mathrm{MIN}}$ and maximum $B_{\delta l\max \mathrm{MAX}}$ as written above.

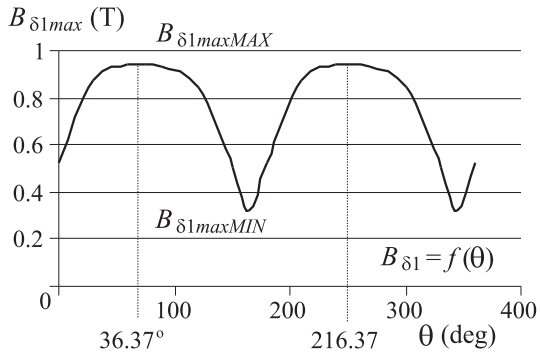

Fig. 7. The amplitudes $B_{\delta l\,\max}$ around the whole air-gap.

The same waveform is rearranged to Fig. 8 (made on the basis of Fig. 4), where one can see the space distribution of $B_{\delta l\,\max}$ in the air-gap. This figure shows that

1) one period of currents corresponds to one cycle movement of the flux density around the whole air-gap periphery, which confirms that it is a two pole machine,
2) in the air-gap there is no circular but an elliptical rotating field,

3) the speed of rotation is not constant: Phasor of $B_{\delta l\,\max}$ is shifted from 0° to 90° in the space between current instants 0° and 156°, and the further shifting by 90° (90° ÷ 180°) is made between current instants 156° and 180°, which means during 24° el. The second half-waveform is repeated in the same way.

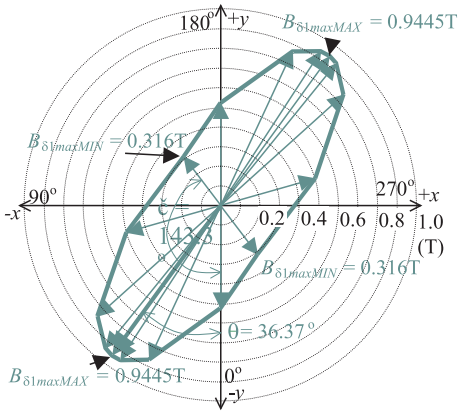

Fig. 8. Space distribution of $B_{\delta l\,\max}$ in the symmetrical air-gap.

3 INVESTIGATION OF RADIAL MAGNETIC FORCES

As it was mentioned above, radial forces, the order of which is given by equation (3), can create noise and vibrations. If $r = 0$, a symmetrically distributed radial force acts on the hollow cylinder of the stator stack. If $r = 1$, the force acts on the rotor as a unidirectional tension, and causes its bending load. If $r = 2, 3, 4, \ldots$, radial forces distort the circular body of the stator to an r-angular frame, and they rotate with an r-times lower speed in comparison with the main field rotation. Obviously the amplitude of the radial forces are decreasing with the increasing r-order, therefore the higher harmonics are less dangerous from the point of view of noise. It results in a procedure, in which the aim is to eliminate the slot harmonics of the lowest order, obviously the first two, that means at $g_S = \pm 1$. Mathematically expressed, for given g_S, at known p and any g_R it must be fulfilled an inequality [1]:

$$\left|(g_S Q_S + p) \pm (g_R Q_R + p)\right| > r\,. \tag{4}$$

If this expression is fulfilled, then stator slot harmonics will be eliminated from the production of radial forces of order less than $(r + 1)$. Solution of eqn. (4) can be used for determination of a suitable number of Q_S and Q_R from the point of view of noiseless operation.

Because in the case of the investigated motor the numbers of Q_S and Q_R are known, it is possible to find the order and magnitude of the produced radial forces. As it is known, the radial forces for air-gap area unit is [1]:

$$f_{\mathrm{rad}} = \frac{B_\delta^2(\Theta, t)}{2\mu_0} \tag{5}$$

In this equation there is given an instantaneous value of air-gap flux density B_δ at time t in the position shifted by θ from the origin, on the circle around the periphery of the air-gap. There is used only μ_0, because it is assumed that $\mu_{F_0} \to \infty$. Nowadays the calculation of f_{rad} forces can be carried out by a computer, by means of FEM, which allows to get data files with $B_\delta = f(\theta, t)$ and their Fourier analysis.

3.1 Symmetrical air-gap

To be able to analyze the presence and values of individual harmonic components in B_δ, it is suitable to apply the theory given above. For the investigated motor, where $Q_S = 24$, $Q_R = 30$ and $p = 1$, on the basis of (1) the stator can create the first four harmonics of order $m = 25$, -23, 49, -47 for $g_S = +1, -1, +2, -2$. The negative sign means that the harmonics rotate opposite to the first one.

The rotor can create the first four harmonics of order $n = 31$, -29, 61, -59 for $g_R = +1, -1, +2, -2$. As it is seen on the cross-section area of the investigated motor (Fig. 2) the slots on the rotor are closed (not opened), therefore its harmonics are suppressed and stator harmonics are dominant. This is seen in Fig. 9, where harmonic components $B_{\delta\nu}$ are shown made on the basis of Fig. 6. Although this spectrum of harmonics is made for currents at $\omega t = 74.6°$, it can be shown that a similar spectrum and values will be gained for further current instants.

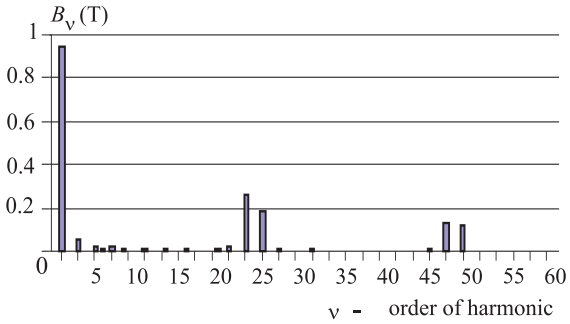

Fig. 9. Harmonic components of the waveform given in Fig. 6.

It results from the solution of equation (4) that Q_S and Q_R of the investigated motor were designed very well, and space harmonics of lower orders are eliminated.

There are dominant above mentioned stator harmonics 23^{rd}, 25^{th}, 47^{th}, 49^{th}. For a symmetrical three-phase motor these harmonics would not be dangerous but for a single phase motor they create a high amplitude (the 23^{rd} is 25 % of the fundamental one) and there are also harmonics which would not appear in the three-phase motor at all (for example 3^{rd} one).

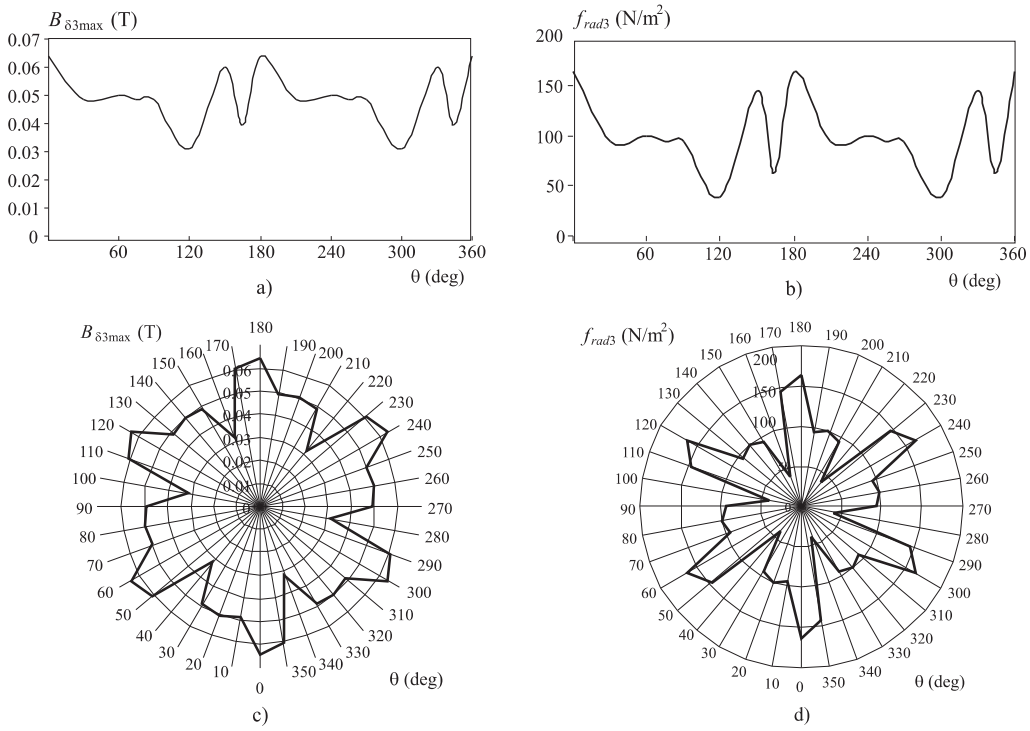

Fig. 10. a) $B_{\delta 3\,\max}$ versus rotor position in electrical degrees b) f_{rad3} versus rotor position in electrical degrees, c) $B_{\delta 3\,\max}$ versus rotor position in mechanical degrees, d) f_{rad3} versus rotor position in mechanical degrees.

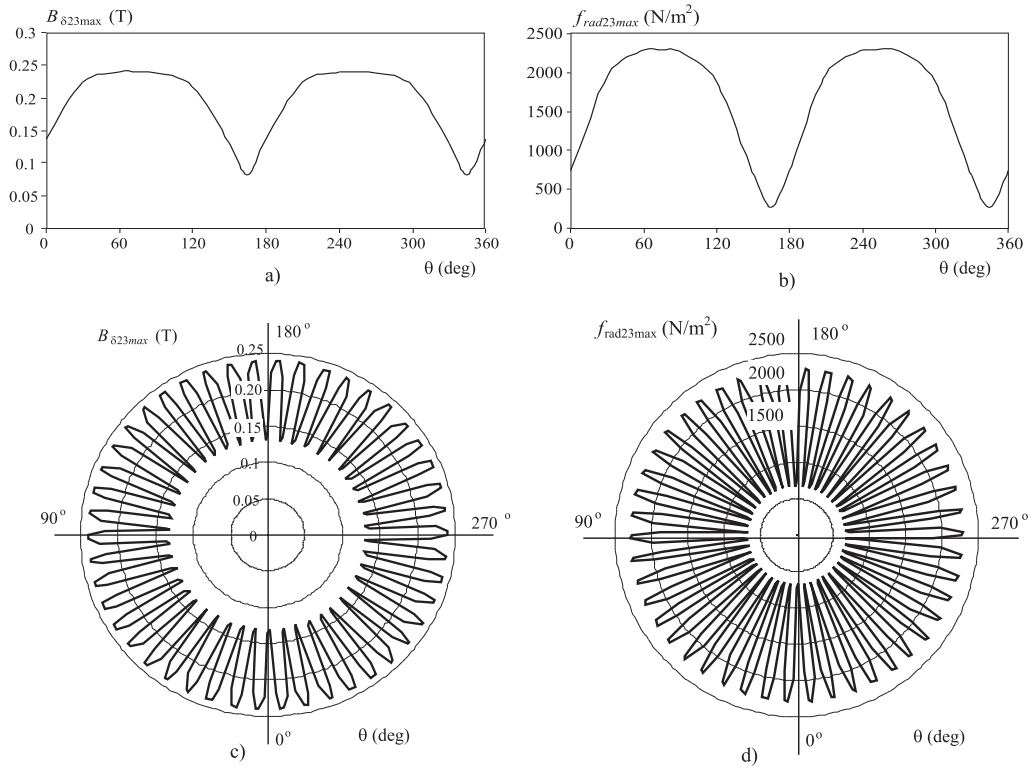

Fig. 11. a) $B_{\delta 23\,\max}$ versus rotor position in electrical degrees b) f_{rad23} versus rotor position in electrical degrees, c) $B_{\delta 23\,\max}$ versus rotor position in mechanical degrees, d) f_{rad23} versus rotor position in mechanical degrees.

In the next, the waveforms of $B_{\delta v}$ and its radial force will be shown on the 360° el., and around the whole air-gap periphery (360° mech.).

It results from the solution of equation (4) that Q_S and Q_R of the investigated motor were designed very well, and space harmonics of lower orders are eliminated.

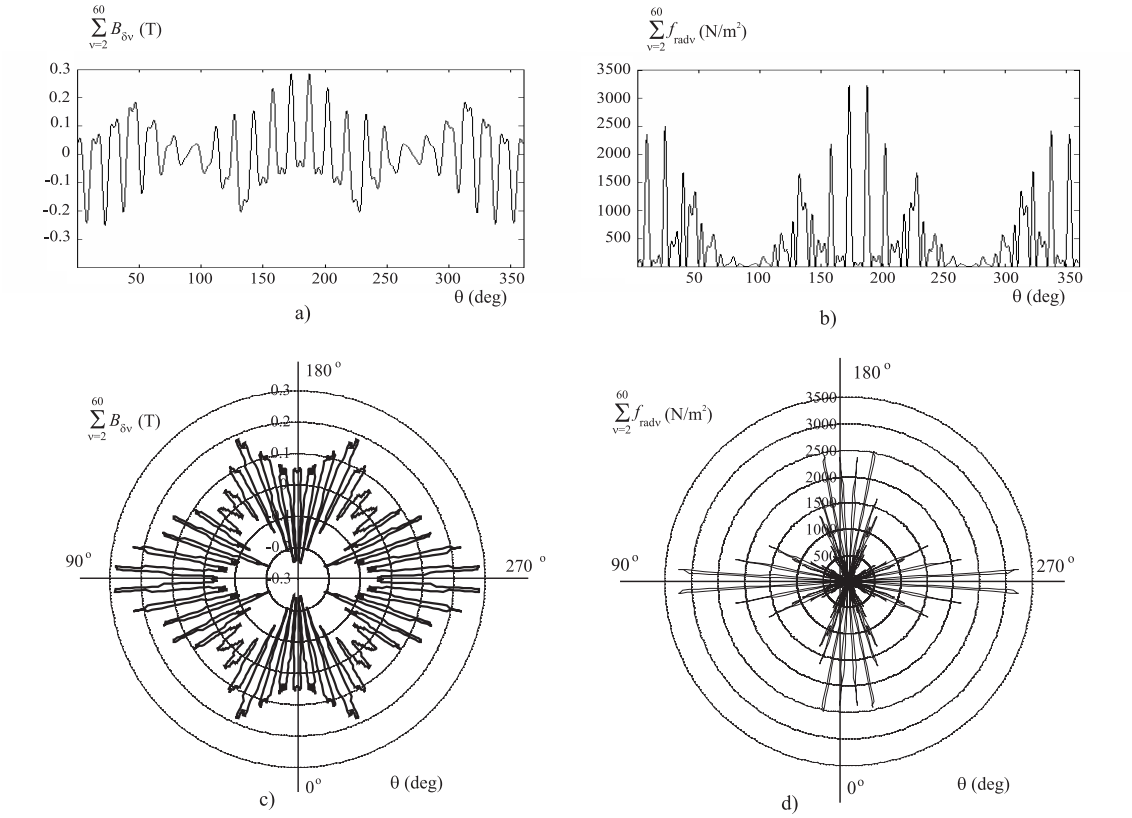

Fig. 12. a) $\sum B_{\delta\nu}$ versus rotor position in electrical degrees b) $\sum f_{\mathrm{rad}\nu}$ versus rotor position in electrical degrees, c) $\sum B_{\delta\nu}$ versus rotor position in mechanical degrees, d) $\sum f_{\mathrm{rad}\nu}$ versus rotor position in mechanical degrees for symmetrical air-gap.

In Fig. 10 there are waveforms of 3^{rd} harmonic, in Fig. 11 the 23^{rd} harmonic components of the air-gap flux density as well as their radial forces.

In Fig. 12 there are the waveforms of $\sum B_{\delta v}$ and $\sum f_{\mathrm{rad}v}$ as the sum of all higher harmonics, excluding fundamental harmonic. This figure will be compared with that made for an asymmetrical air-gap.

3.2 Asymmetrical air-gap

In the previous chapters there was analyzed only the influence of stator and rotor slottings on the air-gap flux density and on the radial magnetic forces. Here an eccentricity of the air-gap will be analyzed from the point of view of radial magnetic forces. Such eccentricity can occur if the stator lamination boring is not perfectly circular, if the rotor is not positioned perfectly in the centre of the stator boring, or if rotor ovality is not perfectly kept.

In Fig. 13 there is seen eccentricity ε and its influence on the air-gap. In this case the eccentricity is located to the axis of the auxiliary winding x-axis. It is valid that $\delta_{\min} + \delta_{\max} = 2\delta_{\mathrm{sym}}$ that means the stator boring and rotor diameter is the same as before, when δ was symmetrical (δ_{sym}).

As it is known [1], this case of eccentricity develops harmonic components of the order $p \pm c$, where c is integer. The strongest harmonics are of the order $p \pm 1$.

In Fig. 14a there is a waveform of the air-gap magnetic flux density at current instant 0° (see also Fig. 4) to show that it is a function symmetrical to the origin of the coordinate system and therefore will contain odd and even harmonic components, as it is seen in Fig. 14b. The waveforms for other current instants will be made similarly but each will be differ from the other in value and position of $B_{\delta\,\max}$ and length of τ_p (see Fig. 15). In all current instants the dominant component is the 2^{nd} one, which is in coincidence with the above predicted order for a 2-pole machine $p \pm 1 = 1 + 1 = 2$. The amplitude of the 2^{nd} harmonics is changing from one current instant to the other and the highest one is at the 0° (Fig. 14b). Besides the 2^{nd}, there are also the harmonics because of stator slotting (23^{rd}, 25^{th}, 47^{th}, 49^{th}).

The fact that $\delta_{\min}$ is in $-x$ axis and $\delta_{\max}$ in $+x$ axis has an influence on the B_δ amplitude as well as on the pole pitch of B_δ, as it is seen in Fig. 15.

From Fig. 15 and at other current instants it can be derived that it is not enough to evaluate the amplitude of the fundamental harmonic, because it does not give a real view of the magnetic field in the air-gap. In fact in $-x$ axis is always high B_δ with a short pole pitch and in $+x$ axis always small B_δ with a longer pole pitch, but the amplitude of fundamental harmonic is always the same with the symmetrical pole pitch.

To compare the fundamental harmonic amplitudes of the air-gap flux density at symmetrical and asymmetrical air-gap, Fig. 16 has been created. As it was mentioned

Table 1.

Current phase	0°		30°		60°		74.6°		90°	
$B_{\delta\max}$	45°	−1.08 T	45°	−1.26 T	45°	−1.33 T	45°	−1.34 T	45°	−1.33 T
position and value	135°	+1.08 T	225°	+1.03 T	225°	+1.16 T	225°	+1.17 T	225°	+1.16 T
Current phase	120°		150°		156°		164.6°		180°	
$B_{\delta\max}$	45°	−1.28 T	45°	−1.07 T	90°	−0.9 T	135°	−0.95 T	45°	+1.08 T
position and value	225°	+1.12 T	225°	+0.8 T	315°	+0.5 T	315°	+0.55 T	135°	−1.08 T

before, there are not seen peculiarities of the air-gap eccentricity.

Therefore the interest must be put to the spectrum and values of air-gap higher harmonics and their influence on the radial forces, as well as the maximum of instantaneous values of B_δ.

In Table 1 there is shown that the moving of $B_{\delta\,\max}$ is very un-equal and non-uniform, more than in the case of a symmetrical air-gap. It is seen that:

1) $B_{\delta\,\max}$ is almost at a constant position between current instant of 0° and 156° (more precisely between 30° and 150°)
2) Between 156° and 180° it runs around the half of periphery,
3) At 180° it has the same positions as at 0° but of opposite polarity,
4) Amplitudes of $B_{\delta\,\max}$ differ in individual half-waveforms and
5) They are not positioned in the span of the regular pole pitch.

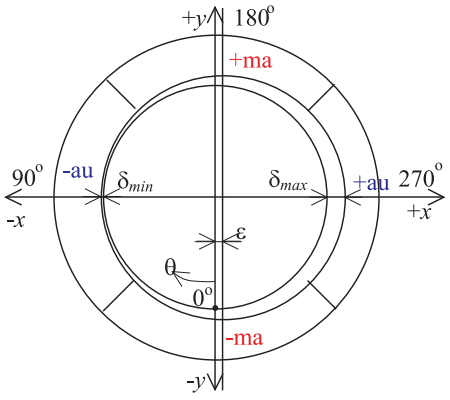

Fig. 13. Illustrative picture showing air-gap eccentricity.

Individual harmonics of B_δ occurring at an asymmetrical air-gap as well as in values of radial forces are evaluated in greater details. As an example is shown the 2nd component which did not occur in the case of $\delta_{\rm sym}$ (see Fig. 17).

To be able to compare the behaviour of the machine at $\delta_{\rm sym}$ and $\delta_{\rm nonsym}$, the sum of all harmonic components $B_{\delta v}$ and $f_{{\rm rad}v}$ excluding fundamental harmonic has been made and it is shown in Fig. 18. It is seen that un-equality of the magnitude and moving of air-gap magnetic flux density is much more significant and it results in much more significant radial forces to which is subjected the stator and rotor cylinder of the single phase motor.

Comparison of Fig. 18c,d and Fig. 12c,d shows the influence of air-gap eccentricity on the radial forces. If there is $\delta_{\rm sym}$, the maximal radial forces achieve the values above 3000 N/m^2 and if there is $\delta_{\rm unsym}$, the radial forces achieve the values above 7000 N/m^2, what is two times more for the defined unsymmetry: $\delta_{\rm sym} = 0.3$ mm, $\delta_{\rm min} = 0.1$ mm, $\delta_{\rm max} = 0.5$ mm. Besides this, the asymmetry of radial forces in x- and y-axis is much more significant in the axis, where asymmetry is made. For here investigated motor, the rotor surface of which is 87 cm^2, the peak value of radial forces with given air-gap eccentricity is 26 N on the whole rotor surface. This results in the conclusion that a symmetrical design of the stator laminated stack, stator boring and rotor ovality is very important for noiseless operation.

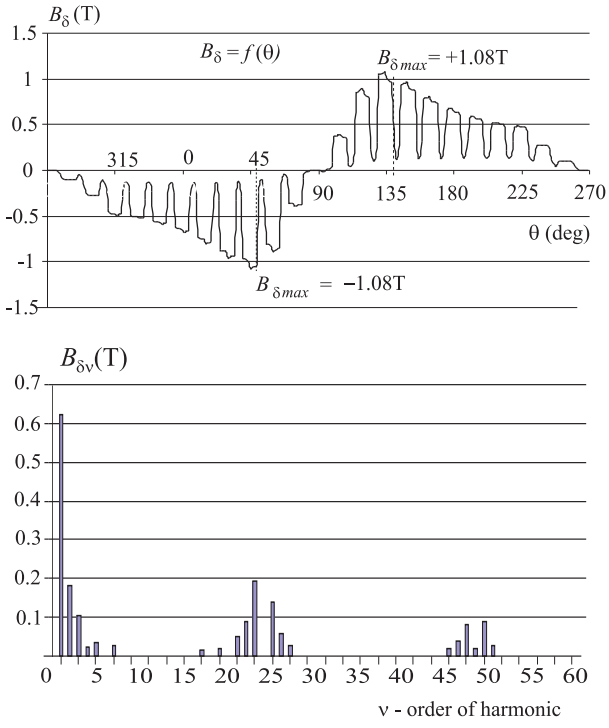

Fig. 14. a) The waveform of air-gap magnetic flux density at the current instant 0° (see Fig. 4), b) odd and even harmonic components of magnetic flux density waveform.

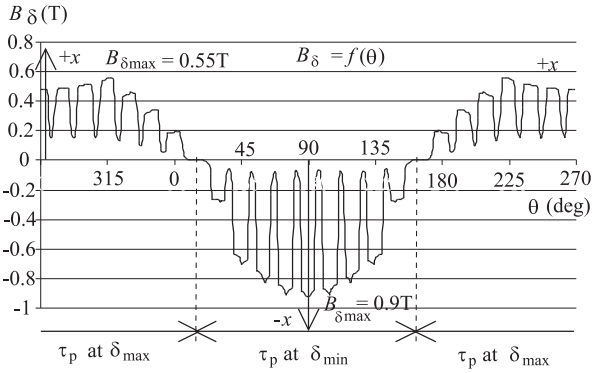

Fig. 15. Magnetic flux density waveform for unsymetrical air-gap.

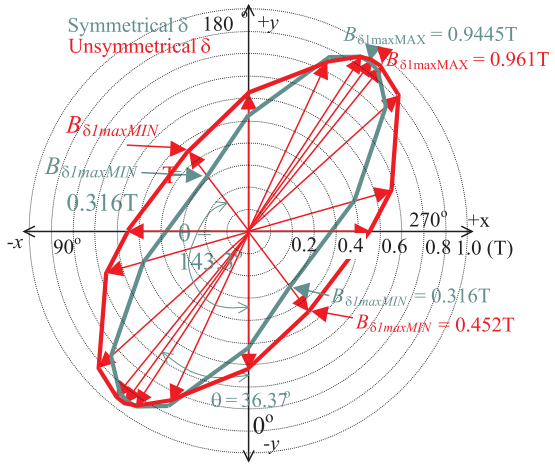

Fig. 16. The comparison of space distribution of the $B_{\delta l\,\max}$ in the symmetrical and unsymmetrical air-gap.

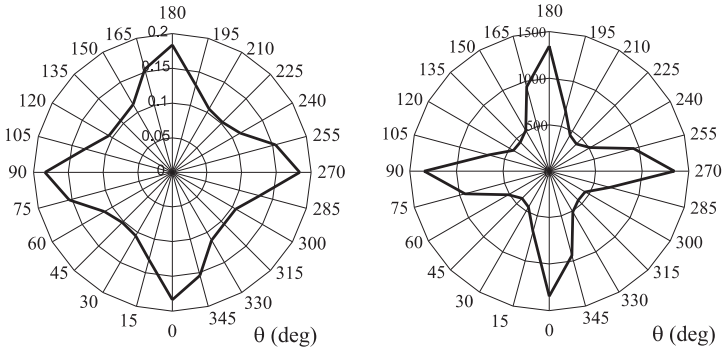

Fig. 17. Flux density and radial force of 2nd harmonic component in unsymmetrical air-gap

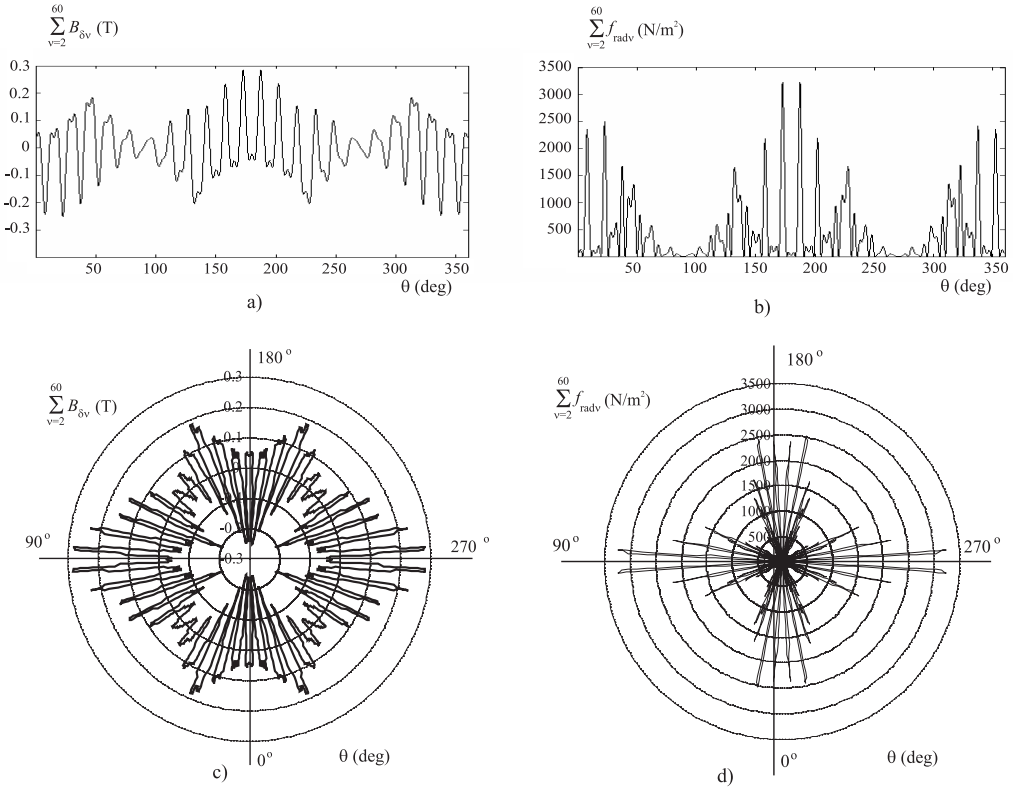

Fig. 18. a) $B_{\delta v}$ versus rotor position in electrical degrees b) $f_{\mathrm{rad}v}$ versus rotor position in electrical degrees, c) $B_{\delta v}$ versus rotor position in mechanical degrees, d) $f_{\mathrm{rad}v}$ versus rotor position in mechanical degrees for unsymmetrical air-gap.

4 CONCLUSION

As it was shown in the paper, the detailed analysis of the form, moving and distribution of magnetic flux density in the cross-section area of the single phase IM results in the confirmation of the theoretical prediction that there is an elliptical magnetic field and that its moving is unequal. Further, the content of higher harmonics has been proved and radial magnetic forces calculated. It was shown that eccentricity of the air-gap has a significant negative influence on the operation of such a motor. Therefore a big interest must be given to the accuracy of the lamination cutting to keep perfectly made stator boring and rotor ovality.

Acknowledgement

This work was supported by the Science and Technology Assistance Agency of the Slovak Republic under the contract No. APVT-20-39602, by VEGA No. 1/2052/05 and VEGA No. 1/3086/06.

References

[1] SZÉKELY, J.—HRABOVCOVÁ, V. To the Design of Frequency Controlled Three phase Induction Motor with Noiseless Operation (K návrhu frekvenčne riadeného trojfázovho asynchrónneho motora s nehlučným chodom): Elektrotechnick obzor Sv. 77, č. 11 (1988), 673–674. (in Slovak)

[2] VOGT, K.: Elektrische Maschinen, Berechnung rotierender elektrischer Maschinen, VEB Verlag Technik Berlin. (in German)

[3] CIGÁNEK, L.: Magnetic Field of Saturated Induction Motor (Magnetické pole nasyceného indukčního motoru), SAV Bratislava, 1965. (in Czech)

[4] HELLER, B.—HAMATA, V.: Additional Fields, Forces and Losses in Induction Motor (Přídavná pole, síly a ztráty v asynchronním stroji), Nakladatelství Československé akademie věd, Praha, 1961.

[5] CHAPMAN, S. J.: Electric Machinery Fundamentals., McGraw-Hill Series in Electrical Engineering, International Edition, 1991.

[6] HAMATA, V.: Noise of Electrical Machines (Hluk elektrických strojů), Academie, 1987. (in Czech)

Received 17 December 2005

Valéria Hrabovcová (Prof, MSc, PhD), graduated in electrical engineering from the University of Žilina in Žilina, gained her PhD in electrical engineering from the Slovak University of Technology in Bratislava in 1985. She is a professor of electrical machines at the University of Žilina, Faculty of Electrical Engineering at undergraduate and postgraduate levels. Her professional and research interests include electronically commutated electrical machines.

Pavol Rafajdus (MSc, PhD, Assistant Professor) graduated in electrical engineering from the University of Žilina, in Žilina in 1995, 2002 and 2005 respectively. At present he is an associate professor at the Faculty of Electrical Engineering, University of Žilina. His research is focused on the reluctance electrical machines properties.